DTU Library

Carbon deposition and sulfur poisoning during CO$_2$ electrolysis in nickel-based solid oxide cell electrodes

Skafte, Theis Løye; Blennow, Peter; Hjelm, Johan; Graves, Christopher R.

Carbon deposition and sulfur poisoning during CO_2 electrolysis in nickel-based solid oxide cell electrodes

Theis Løye Skafte[a, b] (*), Peter Blennow[a], Johan Hjelm[b] and Christopher Graves[b]

[a] Haldor Topsoe A/S, Haldor Topsøes Allé 1, 2800 Kgs. Lyngby, Denmark

[b] Department of Energy Conversion and Storage, Technical University of Denmark, Risø Campus, Frederiksborgvej 399, 4000 Roskilde, Denmark

* To whom correspondence should be addressed: tlsk@dtu.dk, +45 9351 1984

Reduction of CO_2 to CO and O_2 in the solid oxide electrolysis cell (SOEC) has the potential to play a crucial role in closing the CO_2 loop. Carbon deposition in nickel-based cells is however fatal and must be considered during CO_2 electrolysis. Here, the effect of operating parameters is investigated systematically using simple current-potential experiments. Due to variations of local conditions, it is shown that higher current density and lower fuel electrode porosity will cause local carbon formation at the electrochemical reaction sites despite operating with a CO outlet concentration outside the thermodynamic carbon formation region. Attempts at mitigating the issue by coating the composite nickel/yttria-stabilized zirconia electrode with carbon-inhibiting nanoparticles and by sulfur passivation proved unsuccessful. Increasing the fuel electrode porosity is shown to mitigate the problem, but only to a certain extent. This work shows that a typical SOEC stack converting CO_2 to CO and O_2 is limited to as little as 15-45% conversion due to risk of carbon formation. Furthermore, cells operated in CO_2-electrolysis

mode are poisoned by reactant gases containing ppb-levels of sulfur, in contrast to ppm-levels for operation in fuel cell mode.

Keywords

High temperature electrolysis; CO_2 reduction; carbon formation; sulfur poisoning; electrode gradients; mitigation

1. Introduction

The generation and utilization of cheap, renewable electricity is becoming increasingly widespread. The largest sustainable energy sources, solar and wind, are directly linked to the weather and are thus intermittent in nature. As weather changes in the short term and the medium-to-long term due to seasons, production of sustainably sourced energy will vary. Such variable energy production must be balanced with the more constant consumption profile by storing the energy for later use. One promising method of electrical energy storage is by electrolysis of water and/or CO_2 to produce valuable chemicals like hydrogen, synthesis gas, and gaseous and liquid hydrocarbons [1,2]. Compared with conventional low-temperature electrolysis, high-temperature electrolysis with solid oxide electrolysis cell (SOEC) devices offers some distinct advantages. Such devices have high electrical efficiency [3,4] and combined with conventional catalysis they are capable of converting electrical energy into synthetic hydrocarbon fuels [5–7].

With vast excess of electrical energy during some parts of the day and year in the not-too-distant future, the hydrogen economy seems the ideal solution [8]. However, the transition is likely to be excessively costly to implement. An attractive alternative which can take advantage of the already existing infrastructure is a society with a closed CO_2 loop [9].

Production of synthetic hydrocarbon fuels with SOECs and the subsequent Fischer-Tropsch reaction cannot presently compete with cheap oil prices [9]. However, there are niche markets where the SOEC technology can be cost-effectively employed and developed for the long-term scenarios mentioned above. Reduction of CO_2 to CO and O_2 in SOECs is an interesting and seemingly simple process [10]. The products can potentially find use in the chemical industry, military operations where silent production of high purity O_2 is required, or in more unconventional applications such as utilization of the CO_2-rich atmosphere found on Mars [11]. In fact, an SOEC is planned to be brought on the coming 2020-NASA rover-mission for preliminary investigations [12,13]. The initial purpose is oxygen production on location to minimize the amount brought from Earth for a return trip – in fuel combustion, oxygen makes up a large majority of the mass. However, the CO product and/or hydrogen produced by the same electrolysis technology can be used for rocket fuel production, using traditional catalytic fuel synthesis reactions e.g. production of methane from hydrogen and CO_2 or CO. Before a sustainable micro-ecosystem is established, the oxygen produced by the devices can also be used to prepare a breathable atmosphere before human arrival.

CO_2 reduction in a solid oxide cell (SOC) is less studied than H_2O electrolysis and operation in fuel cell mode. Much of the know-how established from decades of solid oxide fuel cell (SOFC) research can be applied directly, but there are also more specific issues, e.g. electrochemically driven carbon formation in Ni containing electrodes. Carbon formation has been extensively studied for steam reforming [14,15], but in the SOC community the issue has mainly received attention during co-electrolysis of CO_2 and H_2O [16,17], and during hydrocarbon fuel cell operation [18–20]. Tao et al. suggested that gradients through the electrode cause carbon formation primarily due to gas diffusion limitations [16,17]. Few studies specifically address carbon deposition during CO_2-electrolysis [21–24]. Some have reported a more severe effect during electrolysis mode compared to fuel cell mode, and Li et al. suspected the direct electrochemical decomposition of CO to C and O^{2-} [24] – an alternative carbon formation pathway than the well-known chemical CO disproportionation (the Boudouard reaction) that could occur

after CO enrichment by CO_2 electrolysis. We are currently investigating the fundamental carbon formation mechanisms in detail in a complementary study [25]. Emphasizing the effect of gradients through the electrode, with a two-dimensional thermal-fluid model, Ni et al. found that the operating potential increases the local current density, which leads to a higher Nernst potential at the electrode|electrolyte-interface and a higher local CO concentration with a fixed CO_2 supply rate [26]. Thus, with a higher operating potential, one could suspect carbon formation to occur locally. Similarly, with an elementary reaction-based model, Shi et al. confirmed the more severe effect at the electrolyte during electrolysis mode [27].

Here, we focus on the technical implications of carbon formation in a full cell during electrolysis, regardless of which fundamental reactions are occurring (electrochemical vs chemical carbon deposition, see Supporting Information section 1 and Fig. S1). We have previously reported a straight-forward *operando* detection method utilizing the voltage-response to a changing current density [28], but we will briefly summarize the arguments for its validity below.

2. Experimental

2.1. Cell testing

Single-cell measurements were performed on Ni-YSZ supported cells with 16 cm^2 active area produced by Haldor Topsoe A/S (YSZ: yttria-stabilized zirconia). The cells had the well-known Ni-YSZ|YSZ|CGO|LSCF-CGO structure (CGO = Gd-doped ceria; LSCF = lanthanum strontium cobalt ferrite). The fuel electrode and electrolyte half-cell was multilayer tape-casted and consisted of a ~300 µm support of Ni-8YSZ, a 10-30 µm active Ni-3YSZ electrode, and a 10-15 µm thick 8YSZ electrolyte. The half-cell and barrier layer was co-sintered and the oxygen electrode was subsequently screen-printed on top. All cells were tested at the Technical University of Denmark (DTU). Further details

about the cells and testing setup can be found in Skafte et al. [28]. Two other cells were tested, produced by DTU with a LSM-YSZ oxygen electrode and nominally the same Ni-YSZ half-cell, but with varying fuel electrode porosity. The difference in porosity estimated from SEM image-analysis and obtained by sintering the half-cell at different temperatures, 1295 °C and 1335 °C, yielded a support porosity of 27% and 23%, and an active electrode porosity of 16% and 13%, respectively. More information about these cells can be found in Ebbesen et al. [29]. Small variations in thickness of the different components and absolute performance of the different cells is not believed to affect the observations reported here. Two of the cells produced by Haldor Topsoe A/S were infiltrated on the fuel side with five cycles of a CGO-nitrate solution (5xCGO), and one cycle of CGO plus five cycles of a Cu-nitrate solution (1xCGO+5xCu). The CGO solution was made by mixing stoichiometric amounts of Ce- and Gd-nitrate salts with water and a surfactant (Triton X-100) to obtain $Ce_{0.8}Gd_{0.2}O_{2-\delta}$. The Cu-solution was made in a similar manner. The cumulative loading for the 5xCGO and the 1xCGO+5xCu cells were approximately 5.7 vol-% and 3.5 vol-%, respectively. This was estimated from the dimensions of the cells, the density of the infiltrated material and the weight-gain per cycle of infiltration. The microstructure of the 1xCGO+5xCu cell after testing is seen in Fig. S2. For more information on these cells and exactly how a Ni-YSZ-supported cell is infiltrated, please see [30].

2.2. Method

By carrying out coking experiments in a CO/CO_2-atmosphere, it is possible to exclude complications from the variety of additional reactions that occur when hydrogen and hydrocarbons are present, such as reverse water-gas shift, methane cracking, or the Bosch reaction. The main carbon deposition reaction considered is the Boudouard reaction, equation 1, however as mentioned earlier and discussed in Supporting Information, direct electrochemical carbon deposition reactions, equation 2 and 3, are also possibilities.

$$2CO \rightarrow CO_2 + C \qquad [1]$$

$$CO_2 \rightarrow O_2 + C \qquad [2]$$

$$CO \rightarrow \tfrac{1}{2}O_2 + C \qquad [3]$$
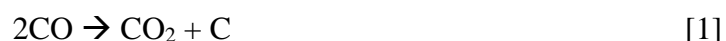
This study investigates the phenomenon of carbon deposition occurring before the expected threshold based on the outlet CO concentration and the thermodynamics of the Boudouard reaction. As an illustration of this issue, a cell was operated in CO/CO_2 with a CO outlet gas concentration just below the Boudouard limit. As seen in Fig. 1a, the cell voltage increased dramatically within just 5 hours of operation, thereby indicating coking conditions in the cell despite being outside the thermodynamically favored region. A method was developed to investigate this further, which is described in more detail in [28]. Electrolysis current was gradually increased in steps over the course of several hours until the voltage became unstable and started increasing (see Fig. 1 in [28]). When this happened, the current was decreased to open-circuit-voltage (OCV) again, and hysteresis in the iV-plot is observed (Fig. 1b). When stopping the current scan well before the Boudouard threshold, the voltage remains stable and no hysteresis is observed. The outlet gas concentration can be calculated using Faraday's law of electrolysis and the ideal gas law, as shown in the Supporting Information.
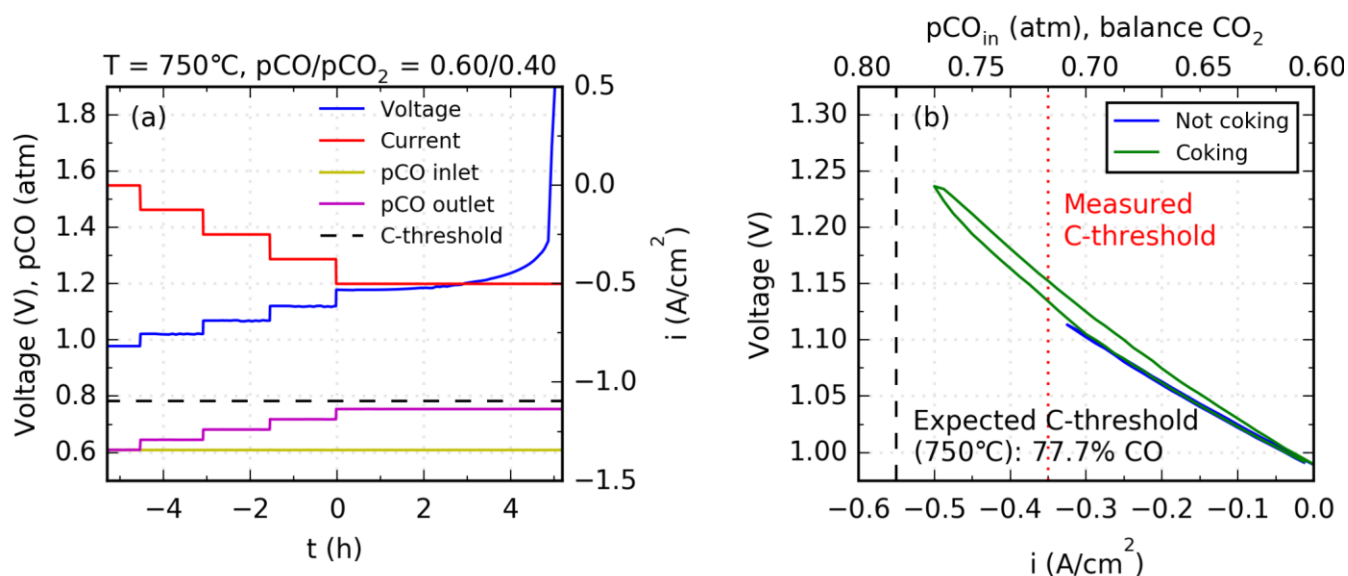
Fig. 1. Cell tests investigating carbon formation: (a) Current density, cell voltage, theoretically calculated pCO gas concentration for the inlet and outlet, and the carbon deposition (Boudouard) threshold for a cell tested in a CO/CO_2-atmosphere. (b) Current-voltage curves in a CO/CO_2 atmosphere. The vertical black line indicates where one would expect the Boudouard threshold to be, based on the outlet gas composition. The vertical red line indicates approximately the position of the measured carbon deposition threshold. Reproduced with permission from ECS Transactions, 68, 3429-3437 (2015). Copyright 2015, The Electrochemical Society.

The operating conditions are only barely crossing into the carbon deposition regime for a short time and the cell thus only suffers minor damage (the cell shown in Fig. 1b is intentionally coked more than regularly for illustrative purposes). Therefore, the experiment can be repeated multiple times on the same cell and statistical confidence in the results are increased significantly.

Further evidence supporting the validity of the method can be found in Skafte et al. [28] and in the supporting information, i.e. measurements of partial oxygen pressure (Fig. S3b), scanning electron microscopy (Fig. S4), and electrochemical impedance spectroscopy (Fig. 5 in [28]). This method is

employed to study the effects of various operational parameters on a commercial cell. The technique was confirmed to reproduce the general trend on three different cell test rigs by different test personnel.

3. Results and discussion

When varying the gas inlet composition, the onset of coking occurs well before the expected Boudouard threshold as calculated from the fuel outlet gas composition. Those calculations are based on average parameters of temperature and current density for the entire cell, and well-mixed gas concentration at the outlet, and not for the local conditions at the reaction sites. The observed deviation of the onset of coking from the expected threshold thus indicates that variations, or gradients, in conditions throughout the cell are the cause of this effect, as was also hypothesized by Tao et al. [16,17]. They showed that with a sufficiently high porosity electrode support layer, carbon deposition was not observed at the same test conditions for which carbon deposition did occur in lower porosity electrodes. Both the gas composition and temperature will vary across the cell as the reactants are converted along the flow direction. Furthermore, the gas composition and temperature will vary within the electrode. When approaching the reaction sites the CO product concentration will increase (gas diffusion limitations) and the temperature will drop (endothermic reaction), which are exactly the conditions that will increase the likelihood of carbon deposition. The fuel electrode overpotential would similarly favor carbon formation at the reaction sites (see Supporting Information). The fact that carbon will deposit at the electrode|electrolyte-interface under electrolysis current has previously been shown experimentally during co-electrolysis by Tao et al. [16,17] and using operando Raman spectroscopy during CO_2 electrolysis by Duboviks et al. [23].

3.1. Effect of operating parameters

The effect of different operating parameters was studied systematically. The effect of fuel electrode porosity was also investigated. This parameter had a large impact on when carbon would form, as the decreased porosity is expected to lead to more severe concentration gradients in the electrode during operation. Current density also showed a high correlation with the onset of carbon formation. The results can be seen in Fig. 2, where each data point for the corresponding cell represents the onset of carbon formation as found using the described method. It is seen from Fig. 2a, that the cell with 30% porosity, operating at -1 A cm^{-2} is limited to an outlet pCO:pCO_2 of 0.55:45 atm, or 23% pCO units below the thermodynamic Boudouard threshold of pCO:pCO_2 0.777:0.223 at the average cell operation temperature. From Fig. 2b, it is seen that the effect is even more severe for cells with low porosity electrodes. Designing a fuel electrode microstructure with small or no gas diffusion resistance could thus increase the carbon tolerance considerably. This could be achieved with a hierarchically oriented electrode such as that reported by Liu et al. [31] or with an electrolyte- or oxygen-electrode-supported design with a thin fuel electrode. However, there may be a porosity threshold above which the beneficial effect of increasing porosity is negligible. Aside from a small gas diffusion resistance, a near zero electrode overpotential would also be required to reach the theoretical threshold, since the overpotential would otherwise decrease the local pO_2 at the reaction site beyond the threshold and carbon would deposit. Based on the thermodynamics of the reaction, carbon is expected to form more easily at lower temperature, but during these experiments it was found that the deviation from the expected threshold was not significantly affected by the temperature (Fig. S5 and Fig. 3 in [28]). Surprisingly, during these tests, both CO_2 utilization (Fig. S6a) and total CO/CO_2 gas flow (Fig. S6b) had little to no impact on the deviation from the expected Boudouard threshold. The current density is naturally strongly linked to the electrode overpotential and the same correlation can thus be observed (Fig. S7).
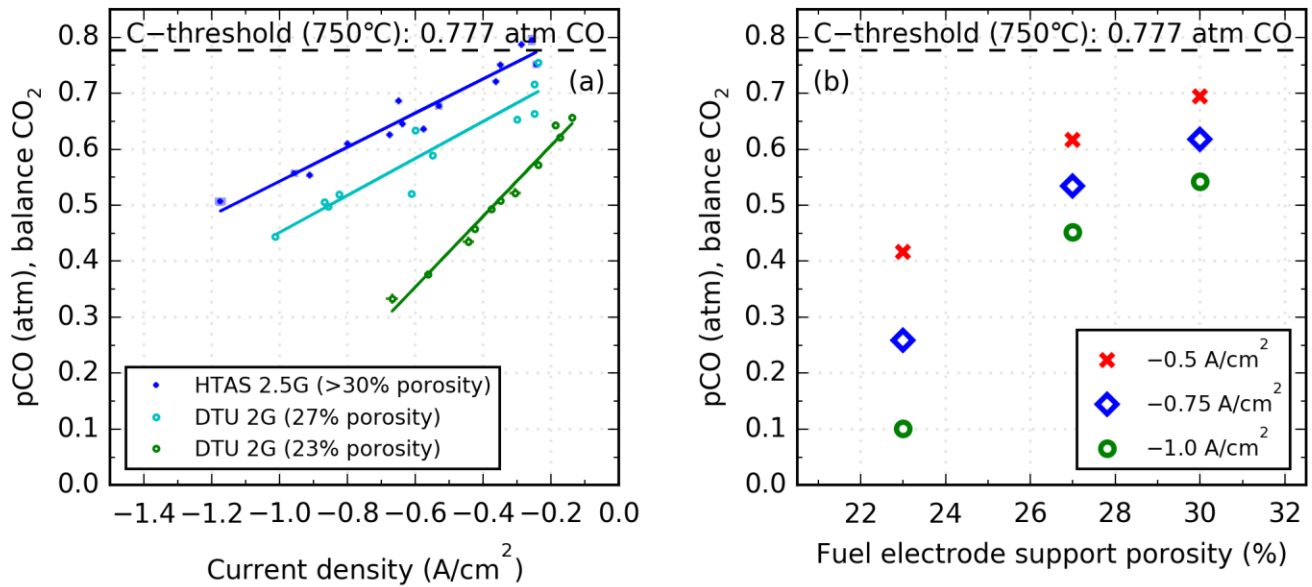
Fig. 2. Three different cells with varying fuel electrode porosity operated at 750 °C with air to the oxygen electrode: The calculated outlet pCO where carbon deposition was found to take place, as found by means of iV-experiments is plotted against (a) current density and (b) porosity of the fuel electrode. Linear regressions in (a) yield the following equations for the >30%, the 27% and the 23% porosity cells respectively; y(x) = 0.305x + 0.847, y(x) = 0.33x + 0.782, and y(x) = 0.632x + 0.733, with coefficients of determination (R^2) of 0.944, 0.888 and 0.981, respectively.

3.2. Modeling verification

The results obtained in this study have been verified by two separate COMSOL multiphysics models. Using a 2D model, Duhn et al. found a high effect of changing the porosity and/or the tortuosity [32]. Likewise, current density was also found to be of high influence on the onset of carbon deposition, in good agreement with this study. Navasa et al. similarly found good agreement between these experimental results and the modeling results of a 3D cell model incorporating kinetic and thermal

effects [33,34]. The carbon activity was shown to be highest at the electrode|electrolyte interface, due to a higher CO concentration and lower temperature on account of the endothermic reaction [35].

The correlation between carbon deposition and current density is of vital importance for a commercial system. One would typically want to increase the current, so as to increase the efficiency and production rate of the stack. Unfortunately, as shown in this study, one will have to balance these parameters with the risk of forming carbon. Increasing the operating temperature to decrease the risk of crossing the Boudouard threshold is often not an option if relatively inexpensive metallic interconnects are used in the stack and long lifetimes are desired. To optimize the operation of the stack, one can use experiments such as these to obtain an expression for the carbon deposition threshold throughout the cell. Similarly, the experiments can be used to confirm full stack multiphysics modeling, where the gradients are more pronounced than for a single cell. Thus, a full size 3D stack model developed at Haldor Topsoe A/S [36] was used to investigate gradients throughout a stack. Including the electrode microstructural effects in a full stack model would be very computational intensive, but the results of the two modeling approaches can be combined to optimize the operating strategy. All in all, one is left with restrictions on the possible operating window coming from gradients in the cell, gradients through the stack and temperature limitations of the interconnect material. The theoretical threshold for the Boudouard reaction in terms of measured outlet pCO and temperature is indicated by a blue line in Fig. 3. When operating the stack below this threshold, one would expect to avoid deposition of carbon inside the cell. However, as shown here and in the multiphysics models mentioned, one must exert extra caution and allow for an additional margin due to gradients and overvoltage as discussed earlier. Thus it is seen that the potential operating window for electrolysis of CO_2 is severely limited by the issue raised in this study. It is noted that the margins indicated in Fig. 3 are merely qualitative and the exact margin required depends on the specific electrode microstructure, cell and stack design, and operating conditions. The method described here can be applied to the specific stack and a possible operating window for that particular stack can be mapped out.
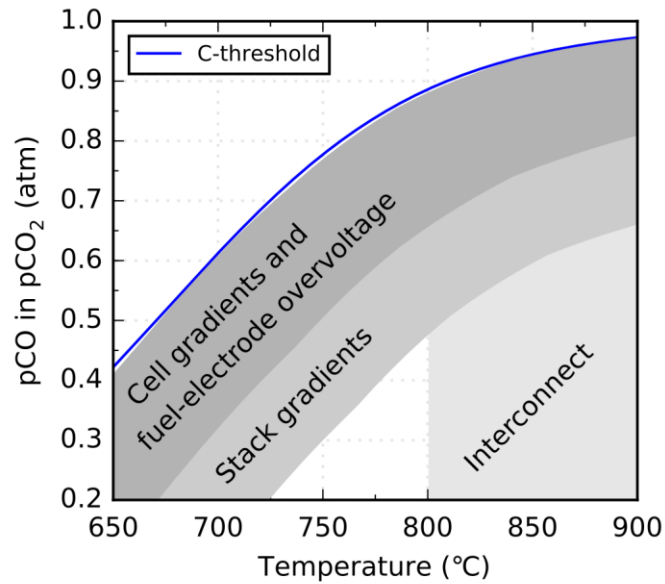
Fig. 3. A qualitative representation of the various restrictions on the possible operating window of a typical CO_2-electrolysis stack. The y-axis refers to the measured outlet pCO of the stack. C-threshold refers to the Boudouard carbon deposition threshold.

3.3. Mitigation

As will be shown in the following, it is extremely difficult to hinder carbon formation while employing the common Ni-YSZ electrode. A lot of work has been done on this issue in the catalysis community [37,38], and there are many methods to consider. One natural way of dealing with the problem would be to use electrodes that do not contain Ni, and DTU is well on its way towards this goal [39,40]. However, presently, due to the many attributes of this well-known catalyst and electrode structure, nearly all established SOC manufacturers employ Ni [41]. Solving this issue without replacing the Ni catalyst would thus be extremely cost-efficient.

If the nickel particles could be completely covered, and stay covered, by for instance CGO or Cu, the coking tolerance may be improved [42]. Both Cu and ceria are known to have low catalytic activity

towards carbon deposition [23,43,44]. However, complete and especially lasting coverage will be difficult to achieve. Moreover, infiltrating a material will also decrease the porosity, which, as shown, is not desirable. Lastly, infiltration as a means of improving coking tolerance has only been successfully demonstrated in CH_4 gas atmospheres in fuel cell mode [42], but not in CO_2-electrolysis mode. Since carbon forms at the electrode surface during fuel cell mode and at the electrode|electrolyte-interface during electrolysis mode, infiltration may not be as useful in the latter case.

Infiltration of the fuel electrode with Cu and CGO was attempted as a carbon deposition mitigation strategy. However, as seen in Fig. 4, the coking tolerance was not improved. However, it is noted that the infiltrated material appears not to have reached and fully covered the active fuel electrode, i.e. up to 10 µm from the electrolyte (Fig. S2b). The active fuel electrode has a lower porosity than that of the support for the tested cells, which could explain the lack of infiltrated material seen here. As explained earlier, the carbon deposition will take place first at the electrode|electrolyte-interface in electrolysis mode, so it is understandable that this approach did not work in this case and would require more optimization of the microstructure (higher porosity) and/or the infiltration solution. In fact, the infiltrated cells showed lower carbon deposition tolerance than the reference. This is most likely due to the lower porosity of the electrode support after infiltration (estimated to 5.7 vol-% and 3.5 vol-% lower for the 5xCGO and the 1xCGO+5xCu, respectively). Comparing the slopes found here to those seen in Fig. 2a, they fall between the cells with 27% and 23% porosity, agreeing well with the estimated 3-6% lower porosity of the infiltrated cells. The negative effect can thus be ascribed primarily to the lower porosity.
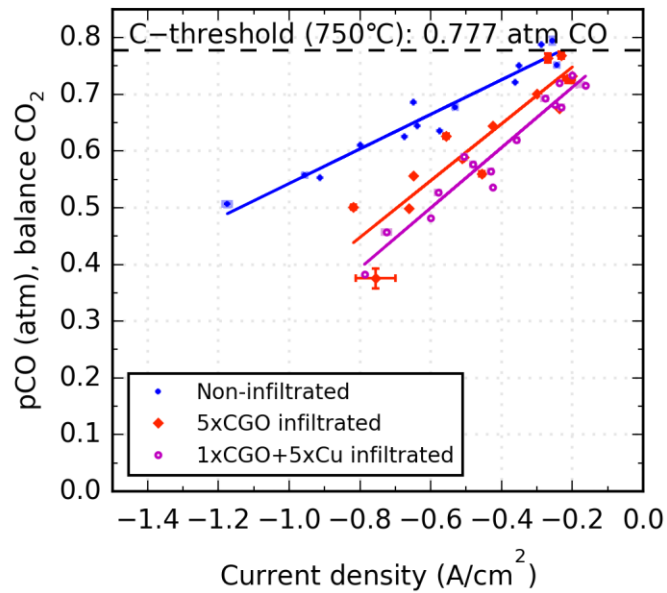
Fig. 4. Two different cells with 30% porosity were infiltrated and operated at 750 °C with air to the oxygen electrode. The calculated outlet pCO where carbon deposition was found to take place, as found by means of iV-experiments, is plotted against current density. Linear regressions yield the following equations for the non-infiltrated, the 5xCGO infiltrated and the 1xCGO+5xCu infiltrated cells respectively; $y(x) = 0.305x + 0.847$, $y(x) = 0.501x + 0.848$, and $y(x) = 0.531x + 0.818$, with coefficients of determination (R^2) of 0.944, 0.827 and 0.941, respectively. Error bars indicate the difference found when repeating the measurement on the same cell.

Another way to cover the Ni particles is by use of sulfur. This is a technique known from heterogeneous catalysis used for steam reforming of methane by means of a Ni catalyst, so-called sulfur passivation [45]. While it is well-known that sulfur is a detrimental impurity in SOFC-mode [38,46–49], little is known about the impact during electrolysis operation, especially with CO and CO_2. However, Ebbesen et al. found remarkable improvements in durability by cleaning the inlet gas during CO_2 electrolysis [50,51]. The effect was ascribed to sulfur in the inlet gases, estimated to 5-8 ppb on account of the specifications from the gas supplier.

Our preliminary investigations on the effect of sulfur on CO_2-electrolysis, show that as little as 5 ppb, as opposed to ppm-levels for SOFC operation [46–49], have a negative effect on the degradation rate. H_2S was flowed on and off for 24 h at a time, increasing the amount each time it was turned on. The degradation rate was estimated for each step and is shown in Fig. 5. Nearly every time H_2S was flowing, the degradation rate increased. Curiously, the exception was while crossing the thermoneutral voltage at approximately 1.5 V. At 20 ppb, the voltage increased dramatically to 1.85 V. Interestingly, the poisoning appeared to be semi-reversible, as the degradation rate returned to the rate observed before adding H_2S, but the absolute voltage did not. Other cell test experiments with 0.5-2 ppm of H_2S, both with and without current running through the cell, confirmed the very strong effect of sulfur poisoning during CO_2-electrolysis. With such concentrations, the cell was completely deactivated within hours.

Two things are important to note in relation to this experiment. Firstly, achieving such low H_2S concentrations required operation of mass-flow-controllers close to the lower recommended threshold for gas flows. Furthermore, additional N_2 was required to dilute the concentration sufficiently. Thus, absolute trust should not be put on the exact values and they should rather be regarded as approximations. Secondly, visual inspection after this test revealed carbon dust on the fuel electrode and similar, or even worse, electrode|electrolyte delamination as shown earlier was found with SEM (see Fig. S8). While the initial effect of H_2S on the degradation rate is not questioned, this delamination along with the sudden jump in voltage after 8 ppb or the large voltage increase after 20 ppb, could be related to carbon formation. Two possible hypotheses explaining these observations are; [a] this could have occurred due to current only flowing through a certain part of the cell, as the rest could have been left electrochemically inactive due to S coverage of the Ni-catalyst. This would increase the local current density and as shown earlier this increases the likelihood of carbon formation. However, this explanation is questionable since the carbon was primarily found to deposit at the fuel inlet part of the cell, the part where the majority of the sulfur is likely to deposit first. [b] Thermodynamically it is expected that when the overpotential on the fuel electrode is high enough, carbon formation will occur (see Supporting

Information). Thus, once the poisoning has increased the overpotential sufficiently, carbon starts forming. This could potentially also have implications on long-term operation, as the overpotential of the fuel electrode will be increasing with time. The local conditions in the electrode will eventually cross the thermodynamic threshold and coke. However, at the time of writing, this has not yet been verified experimentally.
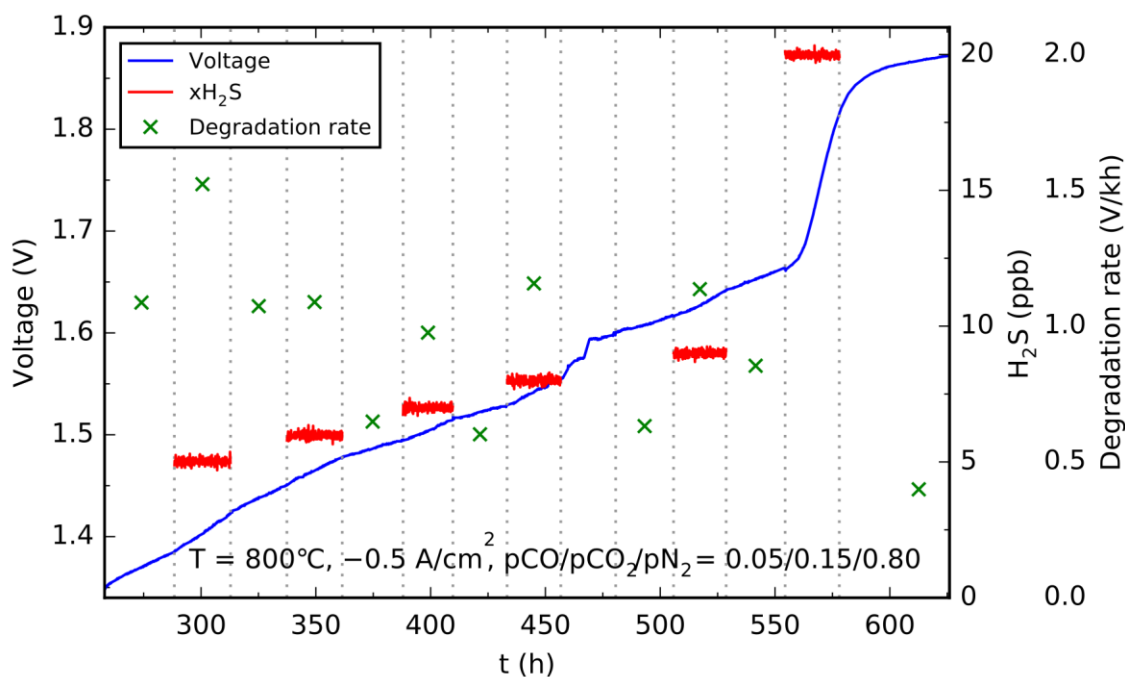

Fig. 5. Voltage while flowing H_2S stepwise from 5 ppb to 20 ppb, and the corresponding degradation rate at each step. Degradation rate with 20 ppb H_2S was 9.1 V/kh. The cumulative amount of H_2S flowed after the 5 ppb, 6 ppb, 7 ppb, 8 ppb, 9 ppb and 20 ppb sessions was respectively 0.03 cm^3/cm^3, 0.07 cm^3/cm^3, 0.11 cm^3/cm^3, 0.16 cm^3/cm^3, 0.22 cm^3/cm^3, and 0.35 cm^3/cm^3, where the latter unit refers to cm^3 of H_2S supplied per cm^3 of electrode.

The sulfur passivation experiment was performed by conducting similar iV measurements as described earlier, after having flowed a certain amount of H_2S. Initial measurements before flowing H_2S showed

that carbon formed at ~70% CO in the outlet, ~8% units lower than expected from global thermodynamic calculations under these conditions – in agreement with the results reported earlier. Considering the dramatic effect of sulfur shown during CO_2-electrolysis, the test was started with flowing a small amount of H_2S into the cell, 6 ppb for 1 min. The amount was gradually increased up to what corresponded to having flown 100 ppb H_2S for 56 h. As seen in Fig. 6, at no point did the sulfur have a positive effect on the carbon tolerance. In fact, the carbon tolerance became worse after having flown 0.05 cm^3 H_2S per cm^3 of electrode. Such an amount of H_2S was reached already during the 6 ppb session in Fig. 5, which further increases the likelihood that carbon formed during that test.
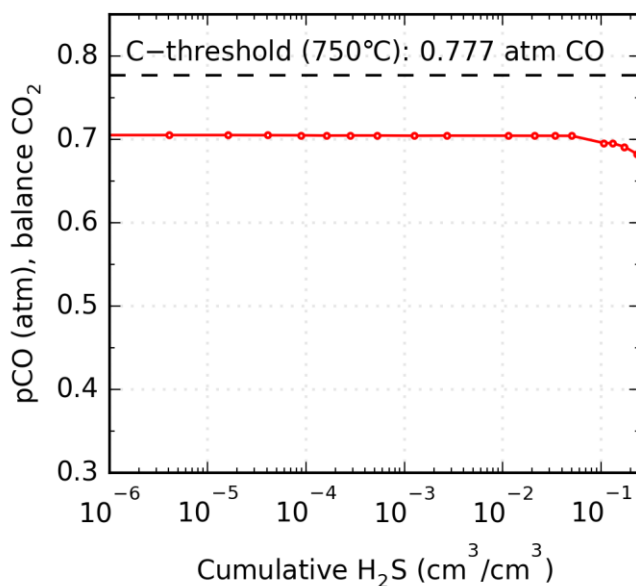

Fig. 6. The outlet gas concentration where carbon deposition was found to take place as found by means of iV-experiments is plotted against the cumulative H_2S flown into the cell. The x-axis unit refers to cm^3 of H_2S supplied per cm^3 of electrode.

4. Conclusions

A simple technique for detecting carbon deposition during CO_2 electrolysis in operating SOCs has been developed. The method was used to estimate the deviation of the measured onset of carbon deposition from that expected from thermodynamic calculations based on averaged cell measurements. The deviation is caused by gradients of temperature, current density and gas concentrations within the cell, as well as the overpotential applied. It was found that both current and fuel electrode porosity had high impacts on the onset of carbon formation.

It is concluded that these gradients throughout the electrode as well as in the entire stack will severely reduce the possible operating window of a commercial SOEC stack during CO_2-electrolysis operation. Depending on the specific cells, stack and operating conditions, the possible CO product output of the stack can be up to ~40% units lower than what would be expected from thermodynamics.

The effect can be mitigated by increasing the fuel electrode porosity, or by adjusting the operational conditions, e.g. operating with lower current density or higher temperature. However, these approaches will not resolve the issue entirely. Three other mitigation strategies were tested, none of which were successful. Replacing the Ni-catalyst is likely to be the only lasting solution, although there are still many possible mitigation strategies that remain to be tested in a SOEC context. Finally, sulfur has been shown to be a significant source of degradation during CO_2-electrolysis with Ni-YSZ electrodes, necessitating the use of thorough gas cleaning to reduce sulfur concentrations to below 5-10 ppb.

5. Glossary

SOEC: Solid oxide electrolysis cell

SOC: Solid oxide cell

SOFC: Solid oxide fuel cell

YSZ: Yttria-stabilized zirconia

CGO: Gd-doped ceria

LSCF: Lanthanum strontium cobalt ferrite

DTU: Technical University of Denmark

OCV: Open-circuit-voltage

Acknowledgments

References

[1]   H. Wu, D. Ji, L. Li, D. Yuan, Y. Zhu, B. Wang, Z. Zhang, S. Licht, A New Technology for Efficient, High Yield Carbon Dioxide and Water Transformation to Methane by Electrolysis in Molten Salts, Adv. Mater. Technol. 1 (2016) 1600092.

[2]   H. Wu, Y. Liu, D. Ji, Z. Li, G. Yi, D. Yuan, B. Wang, Z. Zhang, P. Wang, Renewable and high efficient syngas production from carbon dioxide and water through solar energy assisted electrolysis in eutectic molten salts, J. Power Sources. 362 (2017) 92–104.

[3]   S.D. Ebbesen, S.H. Jensen, A. Hauch, M.B. Mogensen, High Temperature Electrolysis in Alkaline Cells, Solid Proton Conducting Cells, and Solid Oxide Cells, Chem. Rev. 114 (2014) 10697–10734.

[4]   A. Hauch, S.D. Ebbesen, S.H. Jensen, M. Mogensen, Highly efficient high temperature electrolysis, J. Mater. Chem. 18 (2008) 2331.

[5]   S.D. Ebbesen, C. Graves, M. Mogensen, Production of synthetic fuels by co-electrolysis of steam and carbon dioxide, Int. J. Green Energy. 6 (2009) 646–660.

[6]   S.H. Jensen, P.H. Larsen, M. Mogensen, Hydrogen and synthetic fuel production from renewable energy sources, Int. J. Hydrogen Energy. 32 (2007) 3253–3257.

[7]   I.R. Skov, K. Hansen, P. Sorknæs, J. Xu, D. Connolly, B.V. Mathiesen, The role of electrolysers in energy system - Energy markets, grid stabilisation and transport fuels, 2016.

[8]   G.W. Crabtree, M.S. Dresselhaus, M. V Buchanan, The Hydrogen Economy, Phys. Today. 57 (2004) 39–44.

[9]   C. Graves, S.D. Ebbesen, M. Mogensen, K.S. Lackner, Sustainable hydrocarbon fuels by recycling CO_2 and H_2O with renewable or nuclear energy, Renew. Sustain. Energy Rev. 15 (2011) 1–23.

[10] S.D. Ebbesen, M. Mogensen, Electrolysis of carbon dioxide in Solid Oxide Electrolysis Cells, J. Power Sources. 193 (2009) 349–358.

[11] K. Sridhar, B. Vaniman, Oxygen production on Mars using solid oxide electrolysis, Solid State Ionics. 93 (1997) 321–328.

[12] J.J. Hartvigsen, S. Elangovan, D. Larsen, J. Elwell, M. Bokil, L.J. Frost, L.M. Clark, Challenges of Solid Oxide Electrolysis for Production of Fuel and Oxygen from Mars Atmospheric CO_2, ECS Trans. 68 (2015) 3563–3583.

[13] F.E. Meyen, M.H. Hecht, J.A. Hoffman, Thermodynamic model of Mars Oxygen ISRU Experiment (MOXIE), Acta Astronaut. 129 (2016) 82–87.

[14] M.T. Tavares, I. Alstrup, C.A. Bernardo, J.R. Rostrup-Nielsen, CO Disproportionation on Silica-

Supported Nickel and Nickel-Copper Catalysts, J. Catal. 147 (1994) 525–534.

[15] J.R. Rostrup-Nielsen, I. Alstrup, Innovation and science in the process industry: steam reforming and hydrogenolysis, Catal. Today. 53 (1999) 311–316.

[16] Y. Tao, S.D. Ebbesen, W. Zhang, M.B. Mogensen, Carbon Nanotube Growth on Nanozirconia under Strong Cathodic Polarization in Steam and Carbon Dioxide, ChemCatChem. 4000 (2014).

[17] Y. Tao, S.D. Ebbesen, M.B. Mogensen, Carbon deposition in solid oxide cells during Co-electrolysis of H_2O and CO_2, J. Electrochem. Soc. 161 (2014) F337–F343.

[18] X. Li, M. Liu, J. Lee, D. Ding, L.A. Bottomley, S. Park, M. Liu, An operando surface enhanced Raman spectroscopy (SERS) study of carbon deposition on SOFC anodes, Phys. Chem. Chem. Phys. 17 (2015) 21112–21119.

[19] V. Subotić, C. Schluckner, J. Mathe, J. Rechberger, H. Schroettner, C. Hochenauer, Anode regeneration following carbon depositions in an industrial-sized anode supported solid oxide fuel cell operating on synthetic diesel reformate, J. Power Sources. 295 (2015) 55–66.

[20] V. Subotić, C. Schluckner, H. Schroettner, C. Hochenauer, Analysis of possibilities for carbon removal from porous anode of solid oxide fuel cells after different failure modes, J. Power Sources. 302 (2016) 378–386.

[21] R.C. Maher, V. Duboviks, G.J. Offer, M. Kishimoto, N.P. Brandon, L.F. Cohen, Raman Spectroscopy of Solid Oxide Fuel Cells: Technique Overview and Application to Carbon Deposition Analysis, Fuel Cells. 13 (2013) 455–469.

[22] V. Duboviks, R.C. Maher, M. Kishimoto, L.F. Cohen, N.P. Brandon, G.J. Offer, A Raman spectroscopic study of the carbon deposition mechanism on Ni/CGO electrodes during CO/CO_2 electrolysis, Phys. Chem. Chem. Phys. 16 (2014) 13063.

[23] V. Duboviks, M. Lomberg, R.C. Maher, L.F. Cohen, N.P. Brandon, G.J. Offer, Carbon deposition

behaviour in metal-infiltrated gadolinia doped ceria electrodes for simulated biogas upgrading in solid oxide electrolysis cells, J. Power Sources. 293 (2015) 912–921.

[24] W. Li, Y. Shi, Y. Luo, Y. Wang, N. Cai, Carbon deposition on patterned nickel / yttria stabilized zirconia electrodes for solid oxide fuel cell / solid oxide electrolysis cell modes, J. Power Sources. 276 (2015) 26–31.

[25] T.L. Skafte, Z. Guan, M. Machala, C.B. Gopal, M. Monti, L. Martinez, L. Zhang, E. Stamate, S. Sanna, E. Crumlin, H. Bluhm, M. Garcia Melchor, M. Bajdich, W.C. Chueh, C. Graves, Electrochemically driven carbon deposition from CO_2 on nickel and ceria electrodes: Reaction and inhibition mechanisms, submitted for publication (2017).

[26] M. Ni, Modeling of a solid oxide electrolysis cell for carbon dioxide electrolysis, Chem. Eng. J. 164 (2010) 246–254.

[27] Y. Shi, Y. Luo, N. Cai, J. Qian, S. Wang, W. Li, H. Wang, Experimental characterization and modeling of the electrochemical reduction of CO_2 in solid oxide electrolysis cells, Electrochim. Acta. 88 (2013) 644–653.

[28] T.L. Skafte, C. Graves, P. Blennow, J. Hjelm, Carbon Deposition during CO_2 Electrolysis in Ni-Based Solid-Oxide-Cell Electrodes, ECS Trans. 68 (2015) 3429–3437.

[29] S.D. Ebbesen, X. Sun, M.B. Mogensen, Understanding the processes governing performance and durability of solid oxide electrolysis cells., Faraday Discuss. 182 (2015) 393–422.

[30] T.L. Skafte, J. Hjelm, P. Blennow, C. Graves, Eliminating degradation and repairing damage in solid oxide cell and stack fuel electrodes, submitted for publication (2017).

[31] T. Liu, X. Chen, J. Wu, Z. Sheng, G. Liu, Y. Wang, A highly-performed, dual-layered cathode supported solid oxide electrolysis cell for efficient CO_2 electrolysis fabricated by phase inversion co-tape casting method, J. Electrochem. Soc. 164 (2017) F1130–F1135.

[32] J. Dragsbæk Duhn, A. Degn Jensen, S. Wedel, C. Wix, Modelling of gas diffusion in Ni/YSZ electrodes in CO_2 and co-electrolysis, Fuel Cells, 17 (2017) 442-456.

[33] M. Navasa, C. Graves, C. Chatzichristodoulou, T.L. Skafte, B. Sundén, H.L. Frandsen, A three dimensional multiphysics model of a solid oxide electrochemical cell: A tool for understanding degradation, submitted for publication (2017).

[34] M. Navasa, Three dimensional multiphysics modeling of reversible solid oxide electrochemical cells for degradation studies, Lund University, 2016.

[35] M. Navasa, H.L. Frandsen, T.L. Skafte, B. Sundén, C. Graves, Localized Carbon deposition in solid oxide electrolysis cells studied by multiphysics modeling, submitted for publication (2017).

[36] P. Blennow, J. Rass-hansen, T. Heiredal-clausen, R. Küngas, T.H. Nørby, S. Primdahl, Understanding lifetime limitations in the Topsoe Stack Platform using modeling and post mortem analysis, EFCF 2016 Proc. (2016) 298-304.

[37] C. Liu, J. Ye, J. Jiang, Y. Pan, Progresses in the Preparation of Coke Resistant Ni-based Catalyst for Steam and CO_2 Reforming of Methane, ChemCatChem. 3 (2011) 529–541.

[38] P. Boldrin, E. Ruiz-Trejo, J. Mermelstein, J.M. Bermedez Menendez, T. Ramirez Reina, N.P. Brandon, Strategies for Carbon and Sulfur Tolerant Solid Oxide Fuel Cell Materials, Incorporating Lessons from Heterogeneous Catalysis, Chem. Rev. 116 (2016) 13633–13684.

[39] T.L. Skafte, B.R. Sudireddy, P. Blennow, C. Graves, Carbon and Redox Tolerant Infiltrated Oxide Fuel-Electrodes for Solid Oxide Cells, ECS Trans. 72 (2016) 201–214.

[40] C. Graves, L. Martinez, B.R. Sudireddy, High Performance Nano-Ceria Electrodes for Solid Oxide Cells, ECS Trans. 72 (2016) 183–192.

[41] T.L. Skafte, J. Hjelm, P. Blennow, C. Graves, Quantitative review of degradation and lifetime of solid oxide cells and stacks, EFCF 2016 Proc. (2016) 8-26.

[42] J.G. Lee, O.S. Jeon, H.J. Hwang, J. Jang, Y. Lee, S.H. Hyun, Y.G. Shul, Durable and High-Performance Direct-Methane Fuel Cells with Coke-Tolerant Ceria-Coated Ni Catalysts at Reduced Temperatures, Electrochim. Acta. 191 (2016) 677–686.

[43] S. Wang, G.Q. Lu, G.J. Millar, Carbon Dioxide Reforming of Methane To Produce Synthesis Gas over Metal-Supported Catalysts: State of the Art, Energy & Fuels. 10 (1996) 896–904.

[44] D.J.L. Brett, A. Atkinson, D. Cumming, E. Ramirez-Cabrera, R. Rudkin, N.P. Brandon, Methanol as a direct fuel in intermediate temperature, Chem. Eng. Sci. 60 (2005) 5649–5662.

[45] J.R. Rostrup-Nielsen, Sulfur-passivated nickel catalysts for carbon-free steam reforming of methane, J. Catal. 85 (1984) 31–43.

[46] A. Hagen, J.F.B. Rasmussen, K. Thydén, Durability of solid oxide fuel cells using sulfur containing fuels, J. Power Sources. 196 (2011) 7271–7276.

[47] J.B. Hansen, Correlating Sulfur Poisoning of SOFC Nickel Anodes by a Temkin Isotherm, Electrochem. Solid-State Lett. 11 (2008) B178.

[48] A. Hauch, A. Hagen, J. Hjelm, T. Ramos, Sulfur Poisoning of SOFC Anodes: Effect of Overpotential on Long-Term Degradation, J. Electrochem. Soc. 161 (2014) F734–F743.

[49] J.R. Rostrup-Nielsen, J.B. Hansen, S. Helveg, N. Christiansen, A.K. Jannasch, Sites for catalysis and electrochemistry in solid oxide fuel cell (SOFC) anode, Appl. Phys. A. 85 (2006) 427–430.

[50] S.D. Ebbesen, M. Mogensen, Exceptional Durability of Solid Oxide Cells, Electrochem. Solid-State Lett. 13 (2010) B106.

[51] S.D. Ebbesen, C. Graves, A. Hauch, S.H. Jensen, M. Mogensen, Poisoning of Solid Oxide Electrolysis Cells by Impurities, J. Electrochem. Soc. 157 (2010) B1419-B1429.